Clastosome: A Subtype of Nuclear Body Enriched in 19S and 20S Proteasomes, Ubiquitin, and Protein Substrates of Proteasome

Miguel Lafarga,*[†] Maria Teresa Berciano,*[†] Emma Pena,* Isabel Mayo,[‡] Jose G. Castaño,[‡] Dirk Bohmann,[§] João Pedro Rodrigues,[ǁ] João Paulo Tavanez,[ǁ] and Maria Carmo-Fonseca[ǁ¶]

*Department of Anatomy and Cell Biology, Faculty of Medicine, University of Cantabria, 39011 Santander, Spain; [‡]Department of Biochemistry, Faculty of Medicine, Autonomous University of Madrid, 28029 Madrid, Spain; [§]Center for Cancer Biology, University of Rochester Medical Center, Rochester, New York 14642; and [ǁ]Institute of Molecular Medicine, Faculty of Medicine, University of Lisbon, Lisbon, Portugal

Nuclear bodies represent a heterogeneous class of nuclear structures. Herein, we describe that a subset of nuclear bodies is highly enriched in components of the ubiquitin–proteasome pathway of proteolysis. We coined the term clastosome (from the Greek *klastos*, broken and *soma*, body) to refer to this type of nuclear body. Clastosomes contain a high concentration of 1) ubiquitin conjugates, 2) the proteolytically active 20S core and the 19S regulatory complexes of the 26S proteasome, and 3) protein substrates of the proteasome. Although detected in a variety of cell types, clastosomes are scarce under normal conditions; however, they become more abundant when proteasomal activity is stimulated. In contrast, clastosomes disappear when cells are treated with proteasome inhibitors. Protein substrates of the proteasome that are found concentrated in clastosomes include the short-lived transcription factors c-Fos and c-Jun, adenovirus E1A proteins, and the PML protein. We propose that clastosomes are sites where proteolysis of a variety of protein substrates is taking place.

INTRODUCTION

The proteasome is a large proteolytic complex involved in regulated degradation of intracellular proteins (Coux *et al.*, 1996; Baumeister *et al.*, 1998; Voges *et al.*, 1999). Short-lived proteins such as cell cycle regulators and transcription factors are specifically targeted for proteasome degradation by the ubiquitin-conjugation pathway. Other substrates for this pathway include abnormal soluble proteins from the nucleus and the cytosol, and proteins of the endoplasmic reticulum that have been retro-translocated to the cytosol (Bonifacino and Weissman, 1998). Most protein substrates of the proteasome are marked by covalent ligation to ubiquitin, which then acts as a signal to target the modified substrate for proteolytic degradation.

The ubiquitin signal is generated by a series of dedicated enzymes that recognize the target proteins (Hershko and Ciechanover, 1998). Conjugation of ubiquitin involves the formation of an isopeptide bond between the C-terminal glycine residue of ubiquitin and the ϵ-amino group of a lysine residue of the target protein. Ubiquitination begins with an activating enzyme, E1, that hydrolyses ATP and forms a high-energy thioester between a cysteine of its active site and the C terminus of ubiquitin. The ligation of ubiquitin to the substrate is then carried out by a complex composed of a ubiquitin-protein ligase (E3) and a ubiquitin-conjugating enzyme (E2), with E3 being the major determinant of substrate specificity. Conjugated ubiquitin can be a substrate for further ubiquitination reactions and, indeed, most substrates are modified by multiubiquitin chains in which single ubiquitin molecules are linked via isopeptide bonds (Thrower *et al.*, 2000).

The proteasome is a 26S multimeric enzyme composed of two subcomplexes, the 20S proteasome and the 19S regulator (Bochtler *et al.*, 1999; Voges *et al.*, 1999; Zwickl *et al.*, 2000). The 20S proteasome forms the proteolytic core, whereas the 19S regulator (or PA700) confers ATP dependency and ubi-

quitinated substrate specificity on the enzyme. Current models propose a multistep mechanism for protein degradation by the proteasome. The substrate is initially tethered to the proteasome by specific recognition of its ubiquitin tag; this is followed by interaction of the substrate with the regulatory particle, which exhibits chaperone-like activity and promotes substrate unfolding (Braun *et al.*, 1999); the unfolded substrate is then translocated through a narrow channel to gain access to the proteolytic active sites of the enzyme located within the lumen of the core particle.

Although it has been traditionally thought that multiubiquitin chains are virtually essential to target protein substrates for degradation by the eukaryotic 26S proteasome, recent work unraveled a class of proteins that can be degraded by the proteasome in vivo independently of ubiquitin (Verma and Deshaies, 2000). These include ornithine decarboxylase and the cyclin-dependent kinase inhibitor p21$^{\text{Cip1}}$. More recently, the PML protein was shown to be degraded by the proteasome (Zhu *et al.*, 2001), and whether this process depends on ubiquitination remains an open question.

Immunolocalization and biochemical fractionation studies showed that proteasomes are localized both in the nucleus and in the cytoplasm of eukaryotic cells (Brooks *et al.*, 2000, and references therein). In living yeast cells, 26S proteasomes accumulate predominantly in the nuclear envelope-endoplasmic reticulum network (Enenkel *et al.*, 1998; Wilkinson *et al.*, 1998), and recent data suggest that proteasome localization at these sites is important for proper function (Tatebe and Yanagida, 2000). In contrast, green fluorescent protein-tagged proteasomes appear uniformly distributed throughout the cytoplasm and the nucleoplasm in live human cells (Reits *et al.*, 1997). Within these two compartments proteasomes diffuse rapidly, suggesting that recognition and degradation of substrates result from random collisions between the proteasome and intracellular proteins (Reits *et al.*, 1997). Contrasting with this view, dividing cells show a preferential concentration of proteasomes around spindle microtubules (Amsterdam *et al.*, 1993). This pattern is reminiscent of the behavior of cyclin B, which is degraded by the ubiquitin–proteasome pathway and disappears after a wave that starts at the spindle poles and spreads to the spindle equator (Huang and Raff, 1999). This immediately raises the question of whether association of proteasomes with the spindle contributes to the spatially regulated disappearance of cyclin B at the end of mitosis.

During interphase, proteasomes are responsible for the selective degradation of a number of short-lived nuclear transcription factors whose activity must be tightly regulated, such as nuclear factor-κB, STAT1, and Fos/Jun (Ciechanover *et al.*, 1991; Palombella *et al.*, 1994; Kim and Maniatis, 1996). In face of the increasing evidence showing that compartmentalization of regulatory factors by sequestration plays a key role in nuclear function, we decided to investigate the subnuclear localization of the 26S proteasome. Our results show that although proteasomes are most often diffusely distributed throughout the nucleoplasm, they occasionally concentrate in discrete structures. Electron microscopic analysis revealed that these structures correspond to complex doughnut-shaped nuclear bodies. In addition to 19S and 20S proteasomes, the bodies contain ubiquitin, and a number of proteasome substrates, including the adenovi-
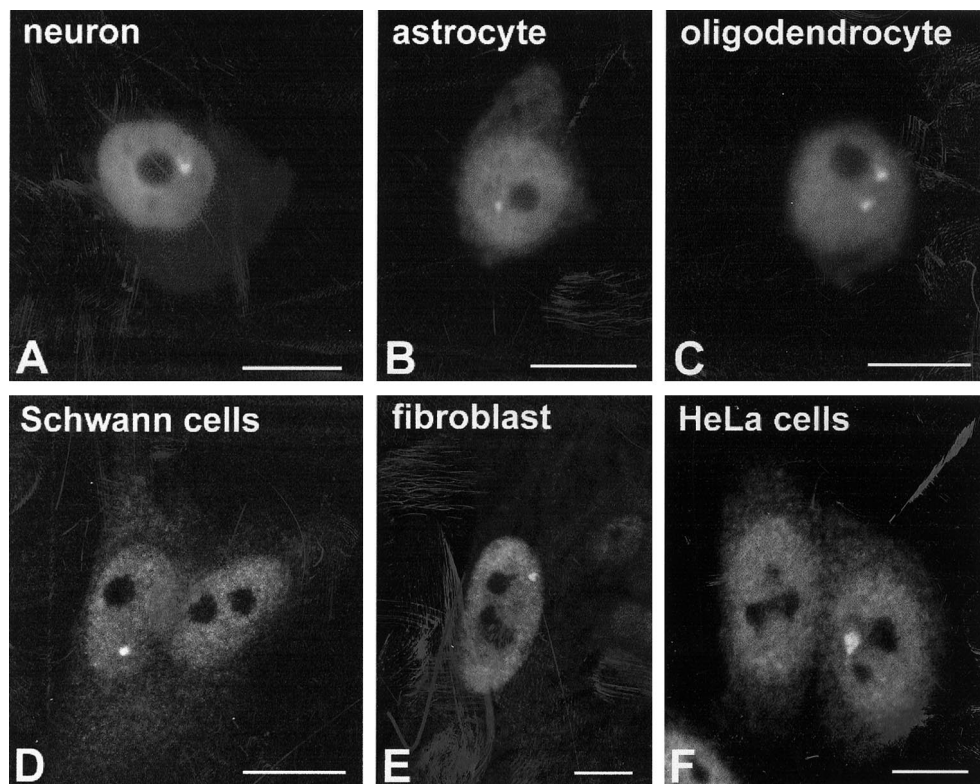

Figure 1. Mammalian cell nuclei contain domains highly enriched in proteasomes. Antibodies directed against the 20S catalytic subunit of the proteasome were used to perform immunofluorescence on a variety of mammalian cell types. These included neurosecretory neurons of the supraoptic nucleus (A), astrocytes (B), and oligodendrocytes (C) obtained from squash preparations of rat hypothalamus, and primary cultures of Schwann cells prepared from rat sciatic nerve (D), human fibroblasts WI-38 (E), and HeLa cells (F). Although anti-20S proteasome antibodies label both nucleus and cytoplasm, staining of the nucleoplasm is more intense. Note the presence of brightly labeled intranuclear structures, of heterogeneous size and shape. Bar, 10 μm.
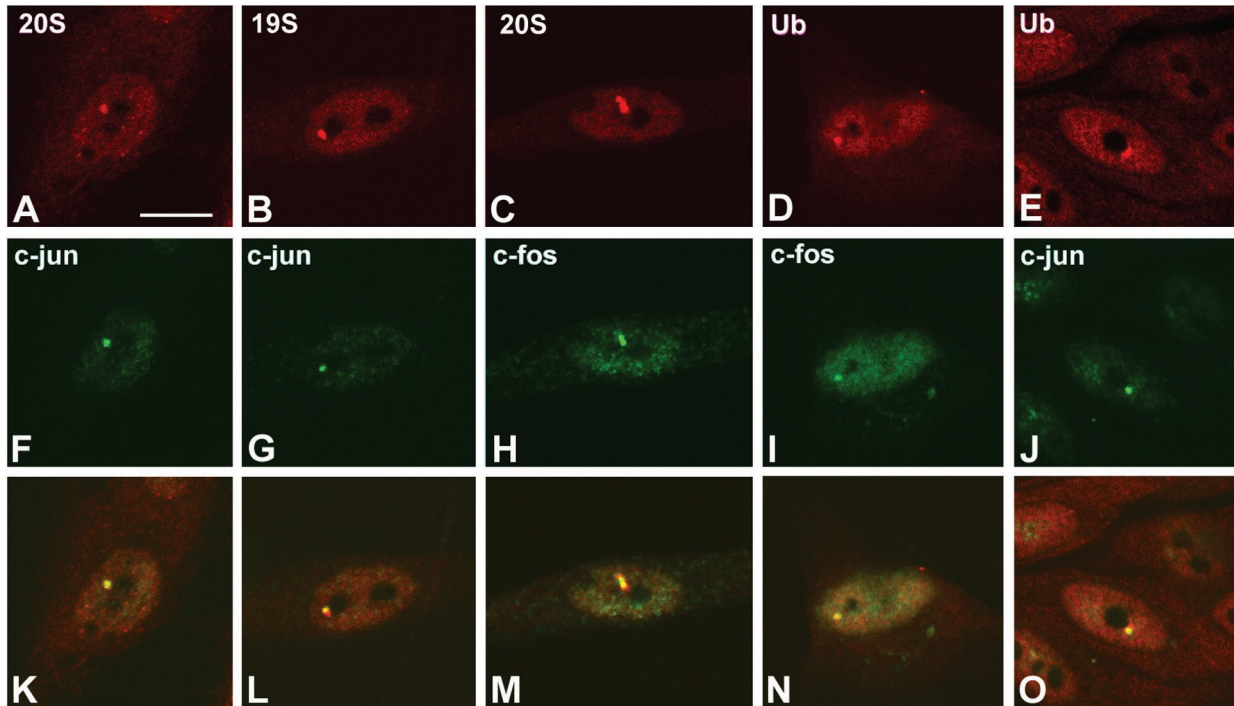
Figure 2. Ubiquitin and proteins degraded by the proteasome colocalize in proteasome-domains. Primary Schwann cells were double-labeled with antibodies directed against 20S proteasome and c-Jun (A and F), 19S proteasome and c-Jun (B and G), 20S proteasome and c-Fos (C and H), ubiquitin and c-fos (D and I), and ubiquitin and c-Jun (E and J). (K–O) Overlay of red and green images. Overlapping of red and green staining produces a yellowish color. Bar, 10 μm.

ral protein E1A proteins, c-Fos and c-Jun, and PML. The results further show that proteasome-containing nuclear bodies are dynamic structures, which assemble transiently under conditions of high proteolysis in the nucleus. We propose the name clastosome (from the Greek *klastos*, broken and *soma*, body) to refer to this nuclear domain.

MATERIALS AND METHODS

Cell Culture

HeLa cells (human epitheloid carcinoma, cervix), and WI-38 cells (human female lung diploid fibroblasts) were grown as monolayers in minimum essential medium supplemented with 2 mM L-glutamine, 50 IU/ml penicillin, 50 mg/ml streptomycin, and 10% fetal calf serum (Invitrogen, Carlsbad, CA). Primary cultures of Schwann cells were prepared as described by Brockes *et al.* (1979). Briefly, sciatic nerves were dissected from 3-d-old Sprague-Dawley rats, and mixed cultures of Schwann cells and endoneurial fibroblasts were maintained in minimum essential medium supplemented with 10% fetal bovine serum for 1 d. To reduce fibroblast contamination, the culture was then incubated for 2 d in the presence of 10^{-5} M cytosine arabinose. On the 4th d the cells were transferred to poly-lysine-coated coverslips and maintained for further 3 d in the presence of 10% fetal bovine serum, 2 μM forskolin, and 20 μg/ml bovine pituitary extract.

Animals

Male, 3-mo-old rats of the Sprague-Dawley strain were kept on a 12-h day, 12-h night lighting regime with lights out at 8:00 AM. All animals were sacrificed by overdose of pentobarbital. To induce an

osmotic stress, animals were given a single intraperitoneal injection of 1.5 M NaCl (18 ml/kg), as described previously (Lafarga *et al.*, 1998).

Immunofluorescence

For indirect immunofluorescence, cultured cells were grown on 10- × 10-mm glass coverslips. The cells were washed twice in phosphate-buffered saline (PBS), fixed with 3.7% formaldehyde (freshly prepared from paraformaldehyde) in PBS for 10 min at room temperature, and subsequently permeabilized with 0.5% Triton X-100 in PBS for 20 min at room temperature. Rats were perfused through the ascending aorta with 3.7% formaldehyde in PBS, pH 7.4, for 15 min at room temperature. Supraoptic nuclei were dissected out of 500-μm-thick hypothalamic slices. These tissue fragments were washed in PBS for 1 h and individually transferred to a drop of PBS on a siliconized slide. Then, a coverslip was applied on top of the slide and the tissue was squashed by percussion with a histological needle. The preparation was then frozen in dry ice, and the coverslip was removed using a razor blade. The slides with adhered neurons were sequentially dehydrated in 96 and 70% ethanol at 4°C for 10 min and rinsed in PBS. Before immunostaining, the samples were sequentially incubated with 0.5% Triton X-100 in PBS for 10 min, 0.1 M glycine in PBS for 30 min, and 0.01% Tween 20 in PBS for 5 min. For immunolabeling, cells were rinsed in PBS containing 0.05% Tween 20, incubated for 1 h with primary antibodies diluted in PBS, washed in PBS containing 0.05% Tween 20, and incubated for 45 min with the appropriate secondary antibodies conjugated to fluorescein (fluorescein isothiocyanate), or Texas Red (Jackson Immunoresearch Laboratories, West Grove, PA). Finally, the coverslips were mounted in VectaShield (Vector Laboratories, Peterborough, United Kingdom) and sealed with nail polish. Confocal
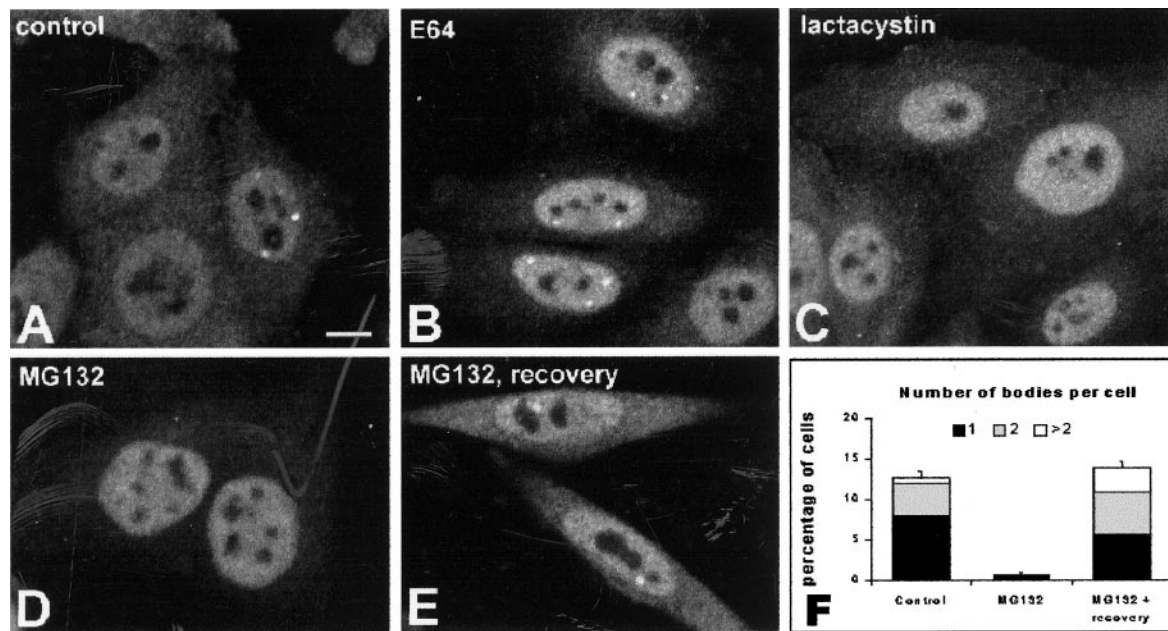
Figure 3. Proteasome-enriched domains disappear in the presence of proteasome inhibitors. HeLa cells were either mock treated (A) or incubated for 3 h in the presence of E64 (B), lactacystin (C), and MG132 (D). The cells depicted in E were allowed to recover for 12 h after treatment with MG132. All cells were immunolabeled with antibodies directed against the 20S catalytic core of the proteasome. Bar, 10 μm. (F) Proportion of cells containing proteasome-enriched domains and the number of bodies per cell were estimated. After treatment with E64, the proportion of cells that contain bodies does not significantly differ from the control population. The graph depicts means $\pm$ SEs (three separate experiments were performed and a total of 300 cells analyzed for each drug treatment).

microscopy was performed with either a laser scanning microscope (LSM 510; Carl Zeiss, Göttingen, Germany) or an MRC-1024 (Bio-Rad, Hercules, CA) by using excitation wavelengths of 488 nm (for fluorescein isothiocyanate) and 543 nm (for Texas Red). Each channel was recorded independently, and pseudocolor images were generated and superimposed.

Immunoelectron Microscopy

Immunoelectron microscopy was performed on cultured Schwann cells or tissue fragments from rat sciatic nerve. Samples were fixed with 4% formaldehyde (freshly prepared from paraformaldehyde) in 0.12 M phosphate buffer, pH 7.4, for 20 min at room temperature, rinsed in phosphate buffer, dehydrated in increasing concentrations of methanol, and embedded in Lowicryl K4 M at −20°C. Ultrathin sections on gold grids were sequentially incubated with 0.1 M glycine in PBS (15 min), 3% bovine serum albumin (BSA) in PBS (15 min), and finally the primary antibody diluted in 1% BSA, 0.1 M glycin in PBS (1 h at room temperature). After washing, the sections were incubated with appropriate secondary antibody conjugated to either 5- or 10-nm gold particles (BioCell, Cardiff, United Kingdom) diluted 1:25 in 0.1% BSA in PBS (45 min at room temperature). Finally, the sections were washed and stained with 10% aqueous uranyl acetate. As controls, sections were treated as described but omitting the primary antibody. Ultrathin sections were examined with an EM208 electron microscope (Philips, Eindhoven, the Netherlands) operated at 60 kV.

Antibodies

Proteasomes were detected using polyclonal antibodies directed against the 20S catalytic core (Arribas *et al.*, 1994; Menqual *et al.*, 1996), and the 19S regulator ATPase subunit 6b (Tbp7; Affiniti

Research Products, Exeter, United Kingdom). Ubiquitin-conjugates were labeled with antibody Z 0458 from DAKO (Glostrup, Denmark), and PML was detected with monoclonal antibody (mAb) PG-M3 from Santa Cruz Biotechology (Santa Cruz, CA). Additionally, the following antibodies were used: mAb 3A3 directed against Hsp70/Hsc70 (MA3-006; Affinity Bioreagents, Golden, CO); mAb M73 raised against E1A proteins (Harlow *et al.*, 1985); mAb 2G9C3 directed against c-Fos (Oncogene Science, Cambridge, MA); mAb anti-c-Jun (J31920; Transduction Laboratories, Lexington, KY); polyclonal antibodies anti-c-Jun (PC06; Oncogene Science); mAb 4G3 (Euro Diagnostica, The Netherlands) directed against the U2B″ snRNP protein (Habets *et al.*, 1989); rabbit polyclonal serum 204.3 anti-coilin (Bohmann *et al.*, 1995); mAb 2B1 anti-SMN (Liu and Dreyfuss, 1996); and rabbit polyclonal antibody C-20 (sc-333; Santa Cruz Biotechnology) directed against Sam68 (Chen *et al.*, 1999). Specificity of antibodies used was confirmed by Western blotting.

Proteolysis Inhibitors

HeLa cells were exposed for 3 h to the proteasomal inhibitors MG132 (50 μM; Calbiochem, San Diego, CA), lactacystin (10 μM; Calbiochem), or the lysosomal protease inhibitor E64 (10 μM; Sigma-Aldrich, St. Louis, MO). Each of these compounds was dissolved in dimethyl sulfoxide (DMSO), and the final concentration of DMSO in the culture medium was 0.25%.

Plasmids and Transfections

Plasmid pE1A contains nucleotides 1–1773 of genomic Ad2 sequences (pML 005 in Bondesson *et al.*, 1994). Plasmids encoding human c-Jun (pMT35), human c-Jun with a deletion of the δ domain (pMT140), and chicken v-Jun (pMT59) were described previously (Treier *et al.*, 1994). HeLa cells were transiently transfected using

FuGene 6 (Roche Applied Science, Indianapolis, IN), according to the manufacturer's instructions.

RESULTS

Mammalian Cell Nuclei Contain Domains Enriched in Proteasomes, Ubiquitin, and Short-lived Transcription Factors

To study the subcellular distribution of proteasomes in mammalian cells, immunofluorescence was performed using polyclonal antibodies specific for the 20S core catalytic component of the 26S proteasome. Characterization of these antibodies was described previously (Arribas et al., 1994; Mengual et al., 1996).

In agreement with other studies, anti-20S antibodies label both the nucleus and the cytoplasm with a diffuse pattern. Similar results were observed in a variety of cell types, including neurons, astrocytes, and oligodendrocytes from rat brain, primary cultured rat Schwann cells, primary human fibroblasts, and HeLa cells. Surprisingly, a fraction of all cellular populations analyzed contained in addition at least one brightly labeled discrete structure in the nucleoplasm (Figure 1). These structures are heterogeneous in size and shape, and although they are occasionally observed at the periphery of the nucleolus, they appear randomly located in the interior of the nucleus.

Double-labeling experiments revealed that 20S, 19S proteasomes and ubiquitin-conjugates colocalize in the brightly labeled nuclear structures (Figure 2). In addition, both c-Jun and c-Fos (two short-lived transcription factors degraded by the ubiquitin–proteasome pathway) accumulate in the proteasome-enriched structures. Proteins that concentrate in discrete nuclear domains but do not colocalize with the proteasome-enriched structures include coilin (Gall, 2000), splicing factors (Misteli, 2000), SMN (Liu and Dreyfuss, 1996), and Sam68 (Chen et al., 1999) (our unpublished data).

Proteasome-enriched Nuclear Domains Are Dynamic Structures

Proteasomal function can be inhibited pharmacologically by covalent or noncovalent modification of its β-subunits. Commonly used proteasome inhibitors include peptide aldehydes and lactacystin. Peptide aldehydes act by forming a reversible hemiacetal adduct with Thr1 on catalytically active β-subunits (Rock et al., 1994; Löwe et al., 1995; Seemüller et al., 1995), whereas the natural product lactacystin irreversibly alkylates Thr1 (Omura et al., 1991; Fenteany et al., 1995; Dick et al., 1996; Groll et al., 1997). To investigate how proteasome inhibitors affect proteasome-enriched nuclear domains, HeLa cells were treated for 12 h with either the peptide aldehyde MG132; lactacystin; a protease inhibitor specific for lysosomal cysteine proteases (E64); or the solvent in which the inhibitors were dissolved (DMSO). Treated cells were fixed and immunolabeled with anti-20S proteasome polyclonal antibodies (Figure 3, A–E). The proportion of cells containing proteasome-enriched domains (or bodies), and the number of bodies present per nucleus was then estimated (Figure 3F).

Incubation with MG132 caused a dramatic disappearance of proteasome-enriched bodies, compared with control cells treated with either solvent only or E64 (a protease inhibitor

that does not interfere with proteasome activity). Because MG132 causes a reversible inhibition of the proteasome, cells treated with this peptide for 12 h were washed and allowed to recover for 12 h. After this recovery period, the proportion of cells containing at least one body was similar to that observed in control cells, but the number of bodies per nucleus was higher. Thus, inhibition of proteasomal function induces the disassembly of proteasome-containing nuclear domains, whereas withdrawal of the inhibition leads to reassembly of these structures. The higher number of bodies observed after inhibitor withdrawal may be the result of increased proteasomal activity on proteins targeted for degradation that accumulated during the period of treatment with the inhibitor.

If the assembly of proteasome-enriched bodies depends on proteasomal activity, it is expected that increasing the cellular levels of proteasome substrates should stimulate the formation of these structures. We therefore thought to estimate the number of bodies in cells under conditions that are known to trigger proteasome-dependent protein degradation.

Transient expression of immediate-early genes such as c-fos is highly inducible as a result of a specific response to growth factors or serum (Bravo et al., 1986). This prompted us to investigate the distribution of proteasomes in response to serum stimulation of cultured cells. Primary human fibroblasts (WI38) were cultured in the presence of 0.1% fetal calf serum for 4 d, transferred to fresh medium containing 20% serum, and analyzed 3 h later. In clear contrast with unstimulated cells, which were largely devoid of proteasome-containing bodies (our unpublished data), cells incubated with serum for 3 h contained one or more bodies
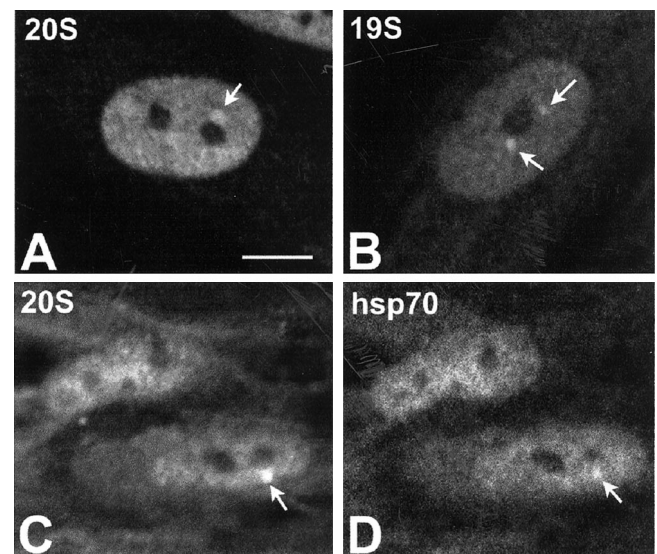

Figure 4. Serum stimulation of fibroblasts induces the appearance of proteasome-enriched domains. Primary human fibroblasts (WI-38) grown in the presence of 0.1% fetal calf serum (FCS) for 4 d were stimulated for 75 min with 20% FCS. Immunofluorescence was performed using antibodies directed against 20S proteasome (A) or 19S proteasome (B). Cells were additionally double-labeled with anti-20S proteasome and anti-Hsp70/Hsc70 antibodies (C and D). Bar, 10 μm.
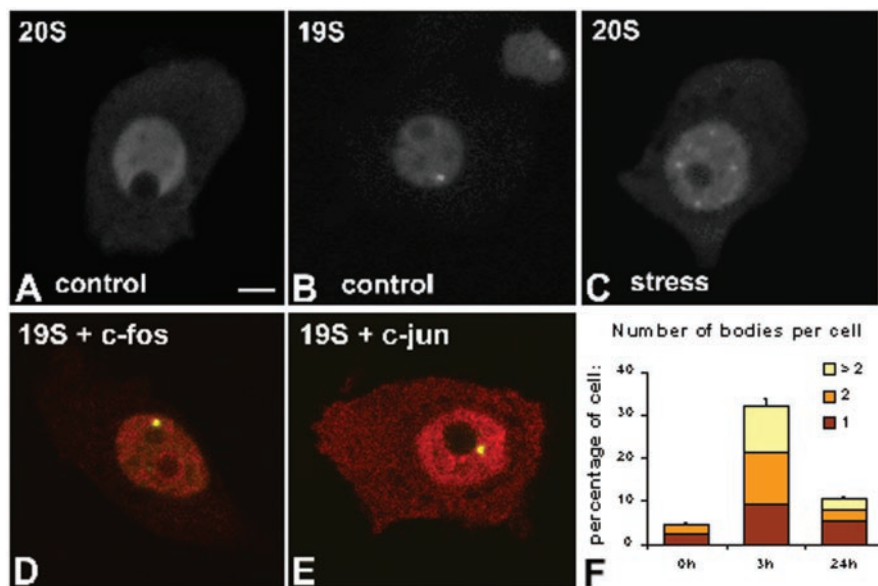
Figure 5. Stress induces the formation of proteasome-enriched domains in rat brain neurons. Hypotalamic neurosecretory neurons were obtained from control animals (A and B) and animals sacrificed 3 h after intraperitoneal injection of an hypertonic saline solution to induce osmotic stress (C–E). Cells were immunolabeled with antibodies directed against 20S proteasome (A and C) or 19S proteasome (B). Cells were additionally double-labeled with either anti-19S proteasome (D, red staining) and anti-c-Fos antibodies (D, green staining), or anti-19S proteasome (E, red staining) and anti-c-Jun antibodies (E, green staining). (D and E) Overlay of red and green images; colocalization produces a yellowish color. Bar, 10 μm. (F) Proportion of neurons containing proteasome-enriched domains and the number of bodies per cell were estimated at 0, 3, and 24 h after saline injection. The graph depicts means $\pm$ SEs (for each time point four animals were sacrificed, and from each animal ~150 neurons were analyzed).

(Figure 4, A–D). As depicted in Figure 4, C and D, these nuclear bodies are also labeled by an mAb (3A3) directed against Hsp70 and Hsc70. Several lines of evidence indicate that the molecular chaperones Hsp70 and Hsc70 interact with the proteasome and are required for the degradation of some proteins (Bercovich et al., 1997; Fischer et al., 1997; Luders et al., 2000; Verma et al., 2000). In fact, substrate unfolding is a kinetically dominant step in proteolysis, and at least certain substrates require extraproteasomal chaperones for efficient degradation (Thrower et al., 2000). Thus, the finding that chaperones Hsp70/Hsc70 localize in proteasome-enriched bodies supports the view that these structures contain functional proteasomes.

It is well established that administration of hypertonic NaCl solutions by intraperitoneal injection in rats causes both osmotic and stressful effects (Ceccateli et al., 1989; Sharp et al., 1991; Xiong and Hatton, 1996). This type of stimulus evokes a transient expression of immediate-early genes such as c-*fos* and c-*jun* in hypothalamic magnocellular neurosecretory neurons (Wang et al., 1997, and references therein). This is followed by an up-regulated synthesis of antidiuretic hormone, a major regulator of body fluid balance (Sherman et al., 1986; Herman et al., 1991; Ding et al., 1994). We have previously shown that in unstimulated animals, the neurosecretory neurons in hypothalamic supraoptic nucleus (SON) are devoid of Fos immunoreactivity. At 30 min after hypertonic saline injection, c-Fos is detected in most neuronal nuclei. Expression of Fos is maximal at 2 h after injection, decreases drastically at 12 h and is no longer detected at 24 h (Lafarga et al., 1998). Consistent with these results, administration of hypertonic saline was shown to induce a transient synthesis of c-*fos* mRNA in SON neurons, which occurs within 5 min and peaks at 30–60 min, whereas expression of Fos protein is maximal at 2 h and decreases thereafter (Sharp et al., 1991; Xiong and Hatton, 1996). In addition to Fos and Jun, a number of other stress-induced proteins are likely to be degraded by the ubiquitin–proteasome pathway in these cells. We therefore counted the number of proteasome-containing bodies in SON neurons from control (unstimulated) animals, and animals sacrificed 3 h after hypertonic saline injection (i.e., when proteolytic destruction of stress-induced proteins is high). The results show that at 3 h after injection there is a drastic increase in the proportion of neurons containing at least one body, as well as a significant increase in the number of bodies per nucleus (Figure 5, A–F). Both Fos and Jun proteins colocalize with 19S and 20S proteasomes in the nuclear body (Figure 5, D and E). At 24 h after injection the number of bodies decreased significantly, although they were still more abundant than in control cells (Figure 5F).

Additional regulators of proteasomal activity are the adenovirus early region 1 transforming proteins. Adenovirus E1A interacts with regulatory components of the 19S proteasome and inhibits the degradation of p53 and E2F transcription factors (Hateboer et al., 1996; Nakajima et al., 1998; Grand et al., 1999; Turnell et al., 2000). Furthermore, E1A is itself a substrate for proteasomal-mediated degradation (Turnell et al., 2000). After transient expression of E1A in HeLa cells, the protein appears exclusively localized in the nucleoplasm with higher concentration in structures of irregular shape and size (Figure 6, A and D). Double-labeling experiments indicate that E1A, proteasomes, and ubiquitin colocalize in the same structures (Figure 6, A–F). Although the proportion of cells containing labeled nuclear bodies is not significantly affected by E1A expression, cells transfected with E1A have more bodies per nucleus than cells that were either nontransfected (Figure 6G) or transfected with control plasmids (our unpublished data). Noteworthy, colocalization of E1A with proteasome and ubiquitin is not complete. There are nuclear bodies labeled by proteasome or ubiquitin antibodies that do not contain E1A (Figure 6E, arrow), and E1A proteins do not always occupy the entire proteasome/ubiquitin-enriched structure (Figure 6F, arrow).

In summary, our data show that the proteasome-enriched nuclear domains contain proteins that are either proteasome substrates or interact with proteasome components. These nuclear domains or bodies disappear
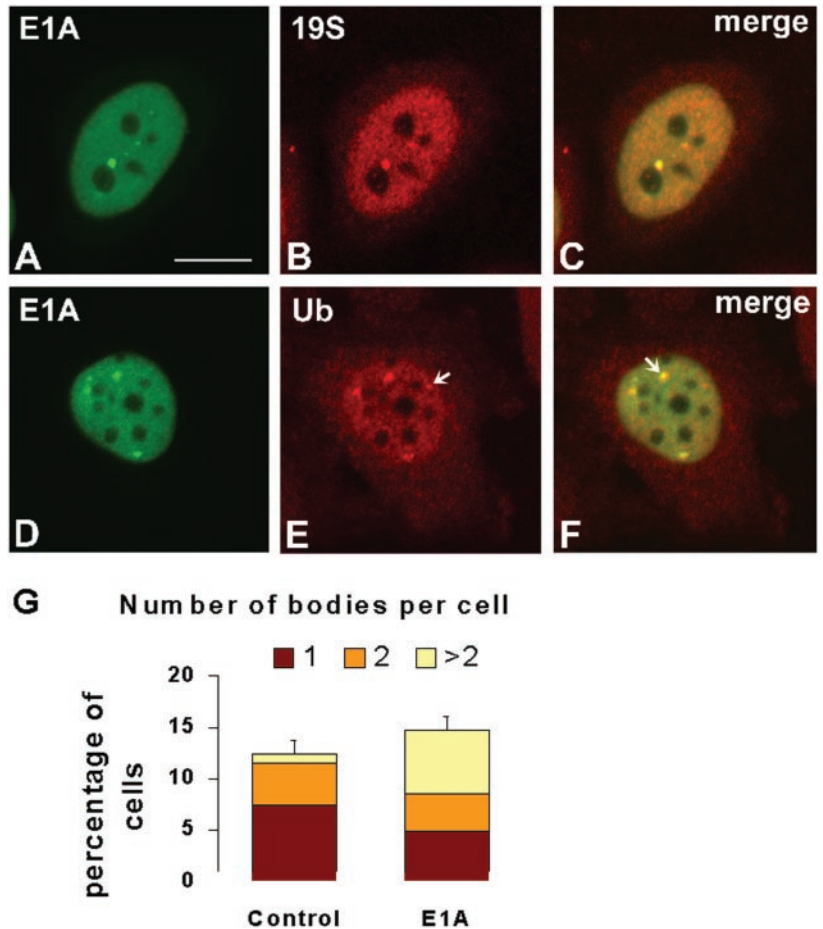
Figure 6. Adenovirus E1A oncoproteins localize in proteasome-enriched domains and stimulate their assembly. HeLa cells transiently transfected with plasmid pE1A, which expresses adenovirus E1A proteins, were double-labeled with anti-E1A antibody M73 (green staining) and either anti-19S proteasome (B and C, red staining) or anti-ubiquitin antibodies (E and F, red staining). (C and F) Overlay of red and green images; colocalization produces a yellowish color. Note that in some cases the E1A proteins occupy only a fraction of the ubiquitin-labeled structures (F, arrow). In E, the arrow indicates a domain enriched in ubiquitin-conjugates but devoid of E1A. Bar, 10 μm. (G) Proportion of transfected cells containing proteasome-enriched domains and the number of bodies per cell were estimated in a total of 300 randomly selected cells. The graph depicts means ± SEs.

when cells are treated with proteasome inhibitors and they form transiently in response to an up-regulation of proteasome activity in the nucleus. Taken together, the data suggest that these structures represent sites where proteasome-dependent proteolysis is taking place. We will refer to them as clastosomes.

Viewed with the Electron Microscope, Clastosomes Correspond to Complex Nuclear Bodies

Anti-20S proteasome and anti-c-Jun antibodies were used to perform immunoelectron microscopy on ultrathin sections of rat brain neurons. As depicted in Figure 7, immunogold particles specifically decorate defined subnuclear structures. These are elongated structures with 0.2–0.5 μm in diameter and 0.5–0.9 μm in length. In cross sections these structures present a characteristic ring-like or doughnut-shaped profile, and occasionally they appear in pairs (Figure 7, A and D). Although no obvious links to nucleoli, chromatin, or any other subnuclear compartment were detected, the proteasome-containing structures are often found in proximity to a nucleolus. On the basis of these morphological features, the proteasome-containing structures correspond to the so-called complex nuclear bodies characterized by the presence of a ring-like "capsule" surrounding a central core with heterogeneous content (Bouteille *et al.*, 1974).

Clastosomes Contain PML

Immunoelectron microscopic analysis with anti-PML antibodies has revealed that nuclear bodies associated with this protein are shaped like a doughnut (Zhong *et al.*, 2000). Given this morphological similarity with clastosomes, we performed double-labeling experiments with anti-PML and either anti-proteasome or anti-ubiquitin antibodies. As illustrated in Figure 8, PML is detected in clastosomes. As observed with E1A proteins (Figure 6), this colocalization is not always perfect. PML tends to occupy only part of a clastosome, indicating that other components are present in the structure. Furthermore, several PML bodies do not stain with proteasome or ubiquitin antibodies. In good agreement with these data, it was reported that at the electron microscopic level PML bodies devoid of proteasomes appear as spheroid aggregates, whereas PML bodies containing proteasomes have the characteristic shell-like or doughnut-shaped structure (Lallemand-Breitenbach *et al.*, 2001).

Clastosomes Are Distinct from Proteasome-containing Nuclear Inclusions

In addition to clastosomes, some cells contain nuclear inclusions intensely labeled by anti-proteasome and anti-ubiquitin antibodies. Nuclear inclusions are very diverse in ap-
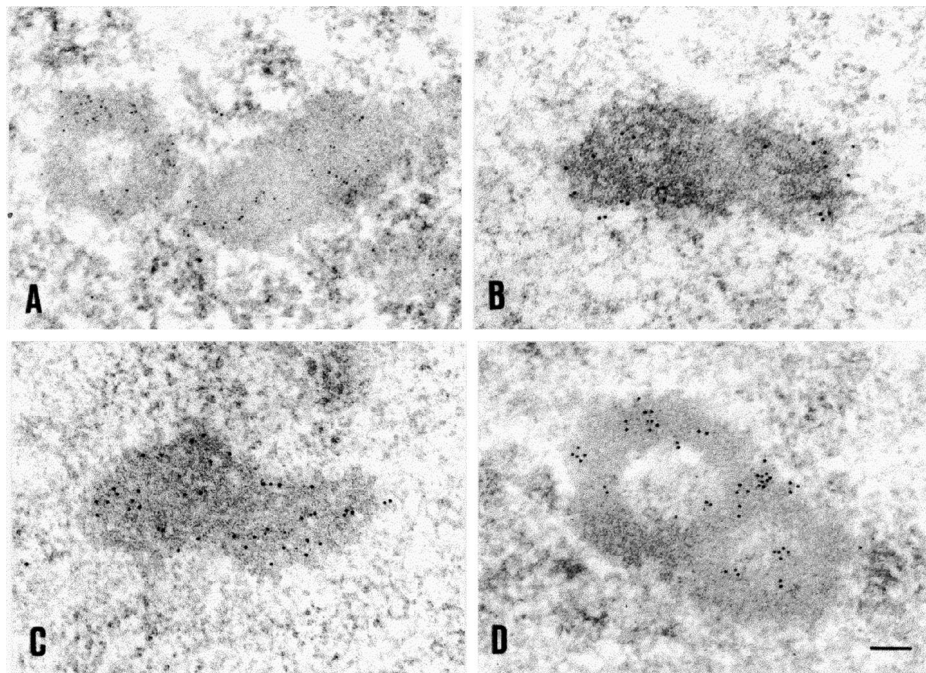
Figure 7. Electron microscopy reveals that proteasome-domains correspond to complex nuclear bodies. Ultrathin sections from primary Schwann cells were immunogold-labeled with antibodies directed against 20S proteasomes (A, 5-nm gold particles), 19S proteasomes (B, 10-nm gold particles), ubiquitin (C, 10-nm gold particles), and c-Jun (D, 10-nm gold particles). Bar, 0.1 μm.

pearance from nuclear bodies and may consist of amorphous, filamentous, or membranous material (Moneron and Bernhard, 1969). In particular, degenerative diseases are often associated with the presence of intranuclear inclusions formed by deposits of aggregated protein in affected neurons and muscle (Galvão *et al.*, 2001; Orr, 2001). Although these deposits are highly enriched in ubiquitylated proteins and components of the proteasome, they are structurally distinct from nuclear bodies and hence they should not be confused with clastosomes. Recent evidence suggests that proteasomes are recruited to these abnormal protein aggregates but because the substrate proteins are tangled into a clump they cannot be efficiently degraded. As a result, the proteasome possibly remains hold onto its prey and consequently fails to degrade the normal protein targets that are constantly being produced in the cell (Bence *et al.*, 2001).

To experimentally address whether nonphysiological deposits of aggregated and ubiquitylated proteins can recruit proteasomes onto intranuclear inclusions, we analyzed the distribution of proteasomes in HeLa cells overexpressing the transcription factor c-Jun. c-Jun is a short-lived protein degraded in the nucleus by the ubiquitin–proteasome pathway (Treier *et al.*, 1994). The protein contains a 27-amino acid segment, the δ domain, which is required for efficient ubiquitination. When the δ domain is deleted, c-Jun is neither ubiquitinated nor degraded (Treier *et al.*, 1994). The oncogenic retroviral counterpart of c-Jun, v-Jun, lacks the δ domain and is not ubiquitinated in vivo. Consequently, v-Jun escapes the mechanism of down-regulation by degradation and the resulting increased stability of the protein most likely contributes to its oncogenicity (Treier *et al.*, 1994).

The overexpressed c-Jun protein forms deposits at the periphery of nucleoli, which are labeled by anti-proteasome antibodies. Viewed with the electron microscope, c-Jun and components of the proteasome are detected in amorphous aggregates that form tangles around nucleoli (Figure 9, A–C). Discrete spheroidal or doughnut-shaped structures containing the exogenously expressed protein are not observed, indicating that overexpressed c-Jun does not assemble into clastosomes. After treatment with proteasome inhibitors, c-Jun is still detected over the tangles of amorphous aggregates (Figure 9C), but labeling of these structures by anti-proteasome antibodies is greatly reduced (Figure 9B). This suggests that in the presence of inhibitors the proteasome is no longer recruited to the c-Jun protein aggregates. We next examined the distribution of proteasomes in HeLa cells overexpressing a deletion mutant of c-Jun lacking the δ domain (c-Jun δ) and v-Jun. The double-labeling experiments depicted in Figure 9, D–I, show that both c-Jun δ and v-Jun form aggregates in the nucleus that fail to recruit the proteasome. Overexpression of unrelated control proteins produced intranuclear aggregates that failed to recruit proteasomes (our unpublished data).

In conclusion, we propose the following model for distribution of proteasomes in the mammalian cell nucleus. All cells contain 19S and 20S proteasomes spread throughout the nucleoplasm. When there is a high demand for proteasome-dependent proteolysis, the excessive protein substrates associated with components of the ubiquitin–proteasome pathway queue up for degradation forming a transient and conserved structure, the clastosome. Once formed, clastosomes recruit more proteins targeted for degradation, thus enhancing the availability of substrates for the proteolytic machine. Under certain pathological or nonphysiological conditions (for example, overexpression), abnormal protein aggregates form in the nucleus. In contrast to the conserved doughnut profile of clastosomes, abnormal deposits of aggregated proteins tend to be amorphous and very irregularly shaped. Proteasomes are recruited and possibly
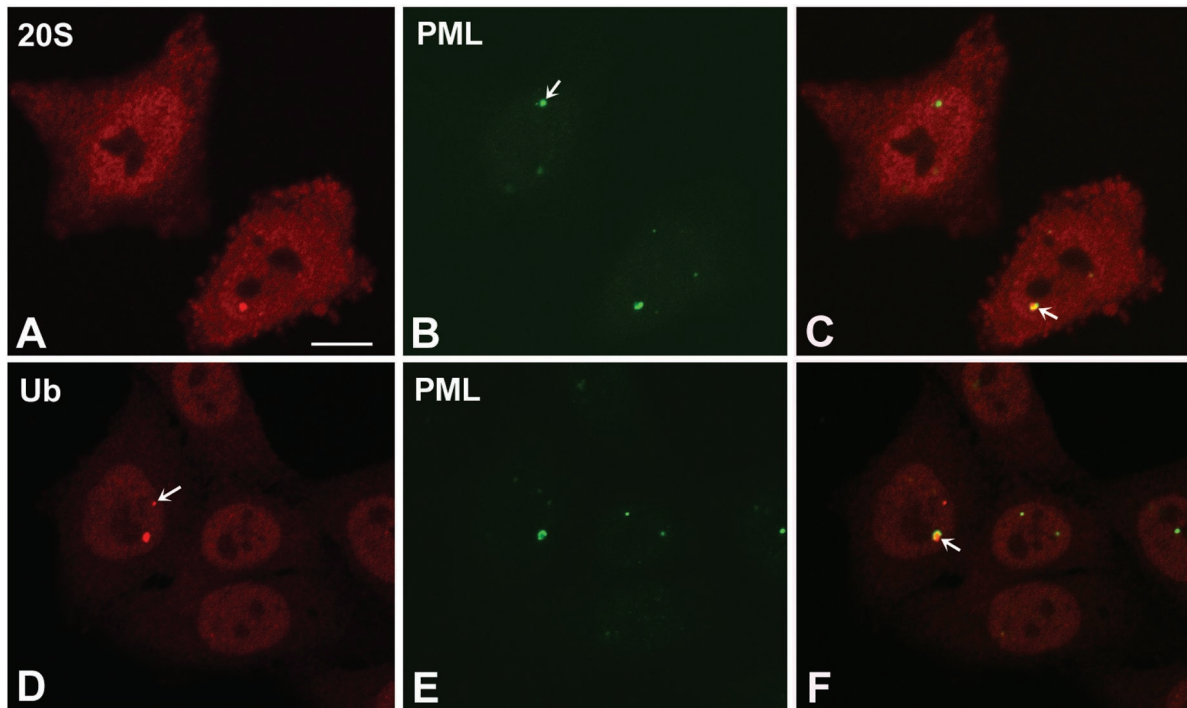
Figure 8. PML protein is present in clastosomes. HeLa cells were double-labeled with anti-PML antibody (green staining) and either anti-20S proteasome (A and C, red staining) or anti-ubiquitin antibodies (D and F, red staining). (C and F) Overlay of red and green images; colocalization produces a yellowish color. Note that PML occupies only a fraction of large clastosomes (C and F, arrow). The arrow in B points to a PML body that does not concentrate proteasomes. In D, the arrow points to a clastosome that contains little, if any, PML. Bar, 10 μm.

trapped within these clumps whenever the aggregates contain proteins recognized by the ubiquitination system.

DISCUSSION

In the nucleus of higher eukaryotes, the majority of short-lived proteins are degraded via the ubiquitin–proteasome pathway (Rock *et al.*, 1994). In contrast with the extensive and detailed knowledge on the structure and enzymatic activity of the proteasome, current understanding of its spatial organization in vivo is lagging behind. Herein, we show that the mammalian cell nucleus contains a specific and conserved domain enriched in proteasomes, which we refer to as the clastosome. The clastosome concentrates 20S and 19S proteasomes, ubiquitin-conjugates and molecular chaperones Hsp70/Hsc70, as well as protein substrates of the proteasome such as c-Fos, c-Jun, PML, and adenoviral E1A proteins. Clastosomes are dynamic structures: they form in response to stimuli that activate proteasome-dependent proteolysis and they disappear when proteasome function is inhibited. This suggests that proteasome-dependent proteolysis is taking place in clastosomes.

When viewed at the electron microscope, clastosomes correspond to nuclear bodies. These structures were first described by De Thé *et al.* (1960), and since then, numerous electron microscopy studies reported the observation of nuclear bodies in a variety of cell types (Bouteille *et al.*, 1967, 1974; Padykula and Clark 1981; Brasch *et al.*, 1989).

On the basis of their structure, nuclear bodies have been classified as either simple or complex (Bouteille *et al.*, 1974). The simple nuclear bodies are small (0.2–0.5 μm) and finely fibrillar, whereas the complex nuclear bodies are larger (0.2–1.2 μm) and enveloped by a peripheral capsule, which gives them a doughnut-shaped appearance. Based on the data presented herein we propose that the doughnut-shaped complex nuclear bodies correspond to clastosomes.

Early electron microscopic studies showed that complex nuclear bodies are normally scarce, but their number increases under certain conditions such as viral infection and hormonal stimulation (Padykula and Clark, 1981; Padykula *et al.*, 1981; Brasch *et al.*, 1989; Brasch and Ochs, 1992). Accordingly, we show herein that clastosomes are absent or scarce in normal cells, indicating that clastosomes are not essential for proteasome function. Under normal conditions misfolded, unassembled, or damaged proteins are rapidly and efficiently degraded by cellular proteasomes. This is probably the reason why clastosomes are not normally detected. In the presence of elevated levels of proteins targeted for proteasome-dependent degradation (for example, in response to viral infection, hormonal stimulation, or stress) these may transiently queue up for proteolysis giving rise to clastosomes. Once formed, clastosomes may act by recruiting additional proteins targeted to the proteasome, thus enhancing the local availability of proteolytic machines for substrate degradation.
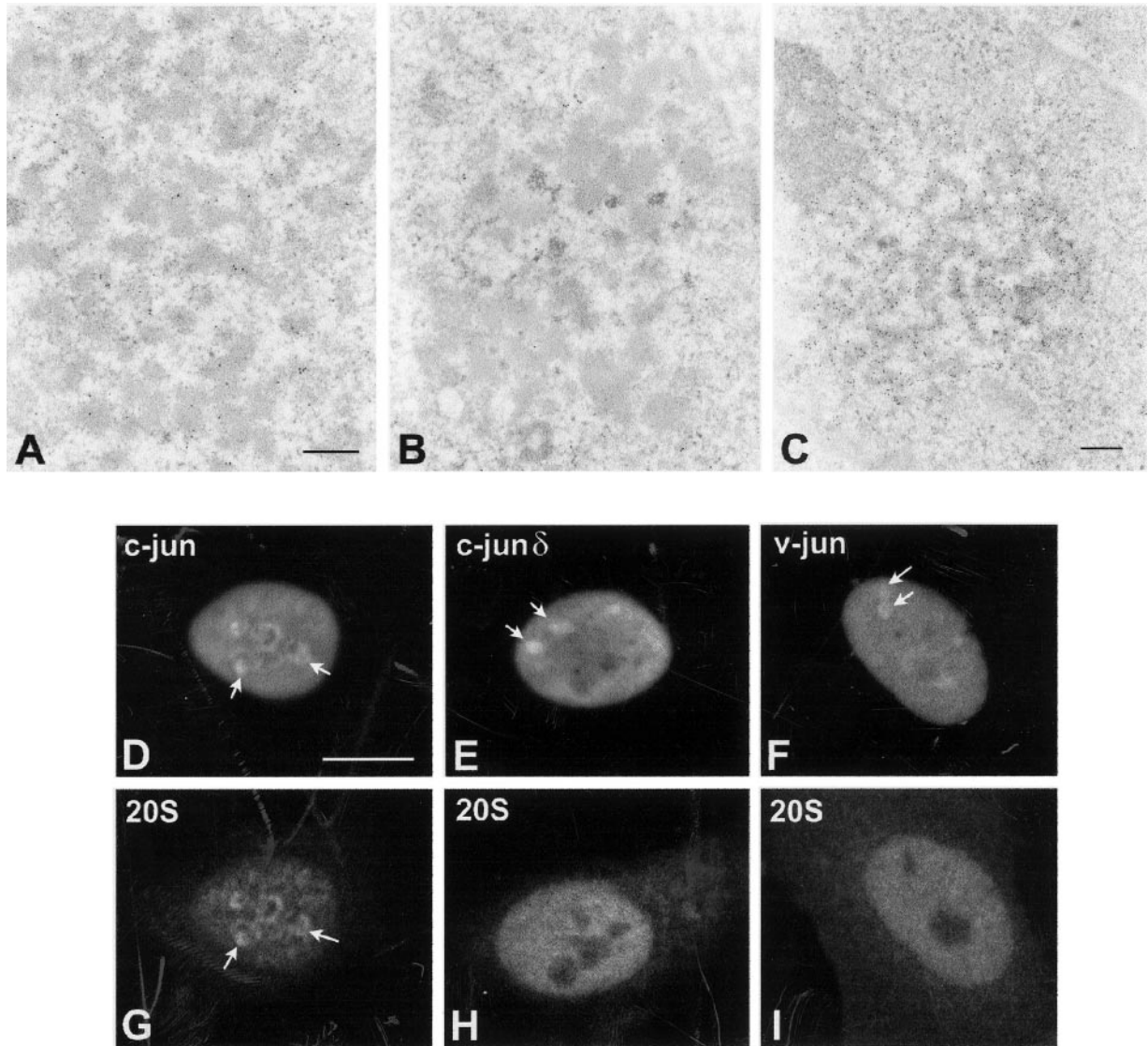
Figure 9. Overexpressed c-Jun protein forms aggregates that recruit proteasomes but are distinct from clastosomes. Ultrathin sections of HeLa cells transiently transfected with a plasmid encoding His$_6$-tagged human c-Jun were immunogold-labeled with anti-20S proteasome (A and B) and anti-His$_6$ antibodies (C). The HeLa cells were either mock treated (A) or incubated for 12 h in the presence of MG132 (B) or lactacystin (C). Bar, 0.3 μm. (D–I) HeLa cells were transiently transfected with a plasmid encoding His$_6$-tagged human c-Jun (D and G), human c-Jun harboring a deletion of the δ domain (E and H), and chicken v-Jun (F and I). The cells were double-labeled with anti-His$_6$ (D–F) and anti-20S proteasome antibodies (G–I). All three forms of the Jun protein produce aggregates in the nucleoplasm (D–F arrows); however, only c-Jun aggregates recruit proteasomes (G, arrows). Bar, 10 μm.

REFERENCES

Amsterdam, A., Pitzer, F., and Baumeister, W. (1993). Changes in intracellular localization of proteasomes in immortalized ovarian granulosa cells during mitosis associated with a role in cell cycle control. Proc. Natl. Acad. Sci. USA *90*, 99–103.

Arribas, J., Arizti, P., and Castaño, J.G. (1994). Antibodies against the C2 COOH-terminal region discriminate the active and latent forms of the multicatalytic proteinase complex. J. Biol. Chem. *269*, 12858–12864.

Baumeister, W., Walz, J., Zühl, F., and Seemüller, E. (1998). The proteasome: paradigm of a self-compartmentalizing protease. Cell *92*, 3673–3680.

Bence, N.F., Sampat, R.M., and Kopito, R.R. (2001). Impairment of the ubiquitin-proteasome system by protein aggregation. Science *292*, 1552–1467.

Bercovich, B., Stancovski, I., Mayer, A., Blumenfeld, N., Laszlo, A., Schwartz, A.L., and Ciechanover, A. (1997). Ubiquitin-dependent degradation of certain protein substrates in vitro requires the molecular chaperone Hsc70. J. Biol. Chem. *272*, 9002–9010.

Bochtler, M., Ditzel, L., Groll, M., Hartmann, C., and Huber, R. (1999). The proteasome. Annu. Rev. Biophys. Biomol. Struct. *28*, 295–317.

Bohmann, K., Ferreira, J.A., and Lamond, A.I. (1995). Mutational analysis of p80 coilin indicates a functional interaction between coiled bodies and the nucleolus. J. Cell Biol. *131*, 817–831.

Bondesson, M., Mannervik, M., Akusjärvi, G., and Svensson, C. (1994). An adenovirus E1A transcriptional repressor domain functions as an activator when tethered to a promotor. Nucleic Acids Res. *22*, 3053–3060.

Bonifacino, J.S., and Weissman, A.M. (1998). Ubiquitin and the control of protein fate in the secretory and endocytic pathways. Annu. Rev. Cell Dev. Biol. *14*, 19–57.

Bouteille, M., Kalifat, S.R., and Delarue, J. (1967). Ultrastructural variations of nuclear bodies in human diseases. J. Ultrastruct. Res. *19*, 474–486.

Bouteille, M., Laval, M., and Dupuy-Coin, A.M. (1974). Localization of nuclear functions as revealed by ultrastructural autoradiography and cytochemistry. In: The Cell Nucleus, vol. I, ed. H. Busch, New York: Academic Press, 3–71.

Brasch, K., Harrington, S., and Blake, H. (1989). Isolation and analysis of nuclear bodies from estrogen-stimulated chick liver. Exp. Cell Res. *182*, 425–435.

Brasch, K., and Ochs, R.L. (1992). Nuclear bodies (NBs): a newly "rediscovered" organelle. Exp. Cell Res. *202*, 211–223.

Braun, B.C., Glickman, M., Kraft, R., Dahlmann, B., Kloetzel, P.-M., Finley, D., and Schmidt, M. (1999). The base of the proteasome regulatory particle exhibits chaperone-like activity. Nat. Cell Biol. *1*, 221–226.

Bravo, R., Burckhardt, J., Curran, T., and Muller, R. (1986). Expression of c-fos in NIH-3T3 cells is very low but inducible throughout the cell cycle. EMBO J. *5*, 695–700.

Brockes, J.P., Fields, K.L., and Raff, M.C. (1979). Studies on cultured rat Schwann cells: I. Establishment of purified populations from cultures of peripheral nerve. Brain Res. *165*, 105–118.

Brooks, P., Fuertes, G., Murray, R.Z., Bose, S., Knecht, E., Rechsteiner, M., Hendil, K.B., Tanaka, K., Dyson, J., and Rivett, J. (2000). Subcellular localization of proteasomes and their regulatory complexes in mammalian cells. Biochem. J. *346*, 155–161.

Ceccateli, S., Villar, M.J., Goldstein, M., and Hokfelt, T. (1989). Expression of c-Fos immunoreactivity in transmitter-characterized neurons after stress. Proc. Natl. Acad. Sci. USA *86*, 9569–73.

Chen, T., Boisvert, F.M., Bazett-Jones, D.P., and Richard, S. (1999). A role for the GSG domain in localizing Sam68 to novel nuclear structures in cancer cells. Mol. Biol. Cell *10*, 3015–3033.

Ciechanover, A., DiGiuseppe, J.A., Bercovich, B., Orian, A., Richter, J.D., Schwartz, A.L., and Brodeur, G.M. (1991). Degradation of nuclear oncoproteins by the ubiquitin system in vitro. Proc. Natl. Acad. Sci. USA *88*, 139–143.

Coux, O., Tanaka, K., and Goldberg, A.L. (1996). Structure and functions of the 20S and 26S proteasomes. Annu. Rev. Biochem. *65*, 801–847.

De Thé, G. de, Rivière, M., and Bernhard, W. (1960). Examen au microscope électronique de la tumeur VX2 du lapin domestique dérivée du papillome de Shope. Bull. Cancer *47*, 569–584.

Dick, L.R., Cruikshank, A.A., Grenier, L., Melandri, F.D., Nunes, S.L., and Stein, R.L. (1996). Mechanistic studies on the inactivation of the proteasome by lactacystin: a central role for clasto-lactacystin β-lactone. J. Biol. Chem. *271*, 7273–7236.

Ding, J.M., Carver, W.C., Terracio, L., and And Buggy, J. (1994). Proto-oncogene c-fos and the regulation of vasopressin gene expression during dehydration. Mol. Brain Research *21*, 247–55.

Enenkel, C., Lehmann, A., and Kloetzel, P.-M. (1998). Subcellular distribution of proteasomes implicates a major location of protein degradation in the nuclear envelope-ER network in yeast. EMBO J. *17*, 6144–6154.

Fenteany, G., Standaert, R.F., Lane, W.S., Choi, S., Corey, E.J., and Schreiber, S.L. (1995). Inhibition of proteasome activities and subunit-specific amino-terminal threonine modification by lactacystin. Science *268*, 726–731.

Fischer, E.A., Zhou, M., Mitchell, D.M., Wu, X., Omura, S., Wang, H., Goldberg, A.L., and Ginsberg, H.N. (1997). The degradation of apolipoprotein B100 is mediated by the ubiquitin-proteasome pathway and involves heat shock protein 70. J. Biol. Chem. *272*, 20427–20434.

Gall, J.C. (2000). Cajal bodies: the first 100 years. Annu. Rev. Cell Dev. Biol. *16*, 273–300.

Galvão, R., Mendes-Soares, L., Camara, J., Jaco, I., and Carmo-Fonseca, M. (2001). Triplet repeats, RNA secondary structure and toxic gain-of-function models for pathogenesis. Brain Res. Bull. *56*, 191–201.

Grand, R.J., Turnell, A.S., Mason, G.G., Wang, W., Milner, A.E., Mymryk, J.S., Rookes, S.M., Rivett, A.J., and Gallimore, P.H. (1999). Adenovirus early region 1A protein binds to mammalian SUG1-a regulatory component of the proteasome. Oncogene *18*, 449–458.

Groll, M., Ditzel, L., Löwe, J., Stock, D., Bochtler, M., Bartunik, H.D., and Huber, R. (1997). Structure of the 20S proteasome from yeast at 2.4 Å resolution. Nature *386*, 463–471.

Habets, W.J., Hoet, M.H., de Jong, B.A., van der Kemp, A., and van Venrooij, W.J. (1989). Mapping of B cell epitopes on small nuclear ribonucleoproteins that react with human autoantibodies as well as with experimentally-induced mouse monoclonal antibodies. J. Immunol. *143*, 2560–2566.

Harlow, E., Franza, B.J., and Schley, C. (1985). Monoclonal antibodies specific for adenovirus early region 1A proteins: extensive heterogeneity in early region 1A products. J. Virol. *55*, 533–546.

Hateboer, G., Kerhoven, R.M., Shvarts, A., Bernards, R., and Beijersbergen, R.L. (1996). Degradation of E2F by the ubiquitin-proteasome pathway: regulation by retinoblastoma family of proteins and adenovirus transforming proteins. Genes Dev. *10*, 2960–2970.

Herman, J.P., Schafer, M.K.-H., Watson, S.J., and Sherman, T. (1991). In situ hybridization analysis of arginine vasopressin gene transcription using intron specific probes. Mol. Endocrinol. 5, 1447–1456.

Hershko, A., and Ciechanover, A. (1998). The ubiquitin system. Annu. Rev. Biochem. *67*, 425–479.

Huang, J.-Y., and Raff, J.W. (1999). The disappearance of cyclin B at the end of mitosis is regulated spatially in *Drosophila* cells. EMBO J. 18, 2184–2195.

Kim, T.K., and Maniatis, T. (1996). Regulation of interferon-gamma-activated STAT1 by the ubiquitin-proteasome pathway. Science *273*, 1717–1719.

Lafarga, M., Berciano, M.T., Garcia-Segura, L.M., Andres, M.A., and Carmo-Fonseca, M. (1998). Acute osmotic/stress stimuli induce a transient decrease of transcriptional activity in the neurosecretory neurons of supraoptic nuclei. J. Neurocytol. *27*, 205–217.

Lallemand-Breitenbach, V., *et al.* (2001). Role of promyelocytic leukemia (PML) sumolation in nuclear body formation, 11S proteasome recruitment, and As2O3-induced P.M.L. or P.M.L/retinoic acid receptor *α* degradation. J. Exp. Med. *193*, 1361–1371.

Liu, Q., and Dreyfuss, G. (1996). A novel nuclear structure containing the survival of motor neurons protein. EMBO J. *15*, 3555–3565.

Löwe, J., Stock, D., Jap, B., Zwickl, P., Baumeister, W., and Huber, R. (1995). Crystal structure of the 20S proteasome from the archaeon *T. acidophilum* at 3.4 Å resolution. Science *268*, 533–539.

Luders, J., Demand, J., and Hohfeld, J. (2000). The ubiquitin-related BAG-1 provides a link between the molecular chaperones Hsc70/Hsp70 and the proteasome. J. Biol. Chem. *275*, 4613–4617.

Mengual, E., Arizti, P., Rodrigo, J., Gimenez-Amaya, J.M., and Castano, J.G. (1996). Immunohistochemical distribution and electron microscopic subcellular localization of the proteasome in the rat CNS. J. Neurosci. *16*, 6331–6341.

Misteli, T. (2000). Cell biology of transcription and pre-mRNA splicing: nuclear architecture meets nuclear function. J. Cell Sci. *113*, 1841–1849.

Moneron, A., and Bernhard, W. (1969). Fine structural organization of the interphase nucleus in some mammalian cells. J. Ultrastruct. Res. *27*, 266–288.

Nakajima, T., Morita, K., Tsunoda, H., Imajoh-Ohmi, S., Tanaka, H., Yasuda, H., and Oda, K. (1998). Stabilization of p53 by adenovirus E1A occurs through its amino-terminal region by modification of the ubiquitin-proteasome pathway. J. Biol. Chem. *273*, 20036–20045.

Omura, S., Matsuzake, K., Fujimoto, T., Kosuge, K., Furuya, T., Fujita, S., and Nakagawa, A. (1991). Structure of lactacystin, a new microbial metabolite which induces differentiation of neuroblastoma cells. J. Antibiot. (Tokyo) *44*, 117–118.

Orr, H.T. (2001). Beyond the Qs in the polyglutamine diseases. Genes and Development *15*, 925–932.

Padykula, H.A., and Clark, J.H. (1981). Nuclear bodies as functional indicators in the target cells of sex steroid hormones. In: The Cell Nucleus, vol. IX, ed. H. Busch, Academic Press, New York, 309–339.

Padykula, H.A., Fitzgerald, M., Clark, J.H., and Hardin, J. (1981). Nuclear bodies as structural indicators of estrogenic stimulation in uterine luminal epithelial cells. Anat. Rec. *201*, 679–696.

Palombella, V.J., Rando, O.J., Goldberg, A.L., and Maniatis, T. (1994). The ubiquitin-proteasome pathway is required for processing the NF-κB1 precursor protein and the activation of NF-κB. Cell *78*, 78–85.

Reits, E.A.J., Benham, A.M., Plougastel, B., Neefjes, J., and Trowsdale, J. (1997). Dynamics of proteasome distribution in living cells. EMBO J. *16*, 6087–6094.

Rock, K.L., Gramm, C., Rothstein, L., Clask, K., Stein, R., Dick, L., Hwang, D., and Goldberg, A.L. (1994). Inhibitors of the proteasome block the degradation of most cell proteins and the generation of peptides presented on MHC class I molecules. Cell *78*, 761–771.

Seemüller, E., Lupas, A., Stock, D., Löwe, J., Huber, R., and Baumeister, W. (1995). Proteasome from *Thermoplasma acidophilum*: a threonine protease. Science *268*, 579–582.

Sharp, F.R., Sagar, S.M., Hicks, K., Lowenstwein, D., and Hisinaga, K. (1991). c-fos mRNA, Fos, and Fos-related antigen induction by hypertonic saline and stress. J. Neurosci. *11*, 2321–31.

Sherman, T.G., McKelvy, J.F., and Watson, S.J. (1986). Vasopressin mRNA regulation in individual hypothalamic nuclei: a northern and in situ hybridization analysis. J. Neurosci. *6*, 1685–1694.

Tatebe, H., and Yanagida, M. (2000). Cut8, essential for anaphase, controls localization of 26S proteasome, facilitating destruction of cyclin and Cut2. Curr. Biol. *10*, 1329–1338.

Thrower, J.S., Hoffman, L., Rechsteiner, M., and Pickart, C.M. (2000). Recognition of the polyubiquitin proteolytic signal. EMBO J. *19*, 94–102.

Treier, M., Staszewski, L.M., and Bohmann, D. (1994). Ubiquitin-dependent c-Jun degradation in vivo is mediated by the delta domain. Cell *78*, 787–98.

Turnell, A.S., Grand, R.J., Gorbea, C., Zhang, X., Wang, W., Mymryk, J.S., and Gallimore, P.H. (2000). Regulation of the 26S proteasome by adenovirus E1A. EMBO J. *19*, 4759–4773.

Verma, R., Chen, S., Feldman, R., Schieltz, D., Yates, J., Dohmen, J., and Deshaies, R.J. (2000). Proteasomal proteomics: identification of nucleotide-sensitive proteasome-interacting proteins by mass spectrometric analysis of affinity-purified proteasomes. Mol. Biol. Cell *11*, 3425–3439.

Verma, R., and Deshaies, R.J. (2000). A proteasome howdunit: the case of the missing signal. Cell *101*, 341–344.

Voges, D., Zwickl, P., and Baumeister, W. (1999). The 26S proteasome: a molecular machine designed for controlled proteolysis. Annu. Rev. Biochem. *68*, 1015–1068.

Wang, K., Guldenaar, S.E.F., and McCabe, J.T. (1997). Fos and Jun expression in rat supraoptic nucleus neurons after acute vs. repeated osmotic stimulation. Brain Res. *746*, 117–125.

Wilkinson, C.R.M., Wallace, M., Morphew, M., Perry, P., Allshire, R., Javerzat, J.-P., McIntosh, J.R., and Gordon, C. (1998). Localization of the 26S proteasome during mitosis and meiosis in fission yeast. EMBO J. *17*, 6465–6476.

Xiong, J.-J., and Hatton, G.I. (1996). Differential responses of oxytocin and vasopressin neurons to the osmotic and stressful components of hypertonic saline injections: a Fos protein double-labeling study. Brain Res. *719*, 143–153.

Zhong, S., Salomoni, P., and Pandolfi, P.P. (2000). The transcriptional role of PML and the nuclear body. Nat. Cell Biol. 2, E85–E90.

Zhu, J., Lallemand-Breitenbach, V, and de Thé, H. (2001). Pathways of retinoic acid-or arsenic trioxide-induced PML/RARα catabolism, role of oncogene degradation in disease remission. Oncogene *20*, 7257–7265.

Zwickl, P., Baumeister, W., and Steven, A. (2000). Dis-assembly lines: the proteasome and related ATPase-assisted proteases. Curr. Opin. Struct. Biol. *10*, 242–250.